LHCHXSWG-INT-2016-xxx
January 14, 2016

LHC Higgs Cross Section Working Group 2 (Higgs Properties)

Pseudo-observables in Higgs physics

Internal note prepared by:
Admir Greljo, Gino Isidori, David Marzocca

We acknowledge contributions and feedback from:
André David, Michael Duehrssen-Debling, Adam Falkowski, Sabine Kraml, Kerstin Tackmann, ...

Disclaimer: this is an incomplete vision of the note (meant only to illustrate the status of the work). Still, any comment/feedback is very welcome.

Contents

1 Introduction

The idea of PO has been formalized the first time in the context of electroweak observables around the Z pole [1]. A generalization of this concept to describe possible deformations from the SM in Higgs production and decay processes has been discussed in Refs. [2–7]. The basic idea is to identify a set of quantities that are

I. experimentally accessible,

II. well-defined from the point of view of QFT,

and capture all relevant New Physics (NP) effects (or all relevant deformations from the SM) without loosing information and with minimum theoretical bias. The last point implies that changes in the underlying NP model should not require any new processing of raw experimental data. In the same spirit, the PO should be independent from the theoretical precision (e.g. LO, NLO, ...) at which NP effects are computed. Finally, the PO are obtained after removing (via a proper deconvolution) the effect of the soft SM radiation (both QED and QCD radiation), that is assumed to be free from NP effects. In the case of observables around the Z pole, the $\Gamma(Z \to f\bar{f})$ partial decay rates provide good examples of PO.

The independence from NP models can not be fulfilled in complete generality. However, it can be fulfilled under very general assumptions. As far as Higgs physics is concerned, the general requirement of Higgs PO is to

III. capture all relevant NP effects in the limit of no new (non-SM) particles below or close to the Higgs mass.

Under this additional hypothesis, the PO provide a bridge between the fiducial cross-section measurements and the determination of NP couplings in explicit NP frameworks.

On a more theoretical footing, the Higgs PO are defined from a general decomposition of on-shell amplitudes involving the Higgs boson –based on analyticity, unitarity, and crossing symmetry– and a momentum expansion following from the dynamical assumption of no new light particles (hence no unknown physical poles in the amplitudes) in the kinematical regime where the decomposition is assumed to be valid. These conditions ensure the generality of this approach and the possibility to match it to a wide class of explicit NP model, including the determination of Wilson coefficients in the context of Effective Field Theories.

The old κ framework [8] satisfied the conditions I and II, but not the condition III, since the framework was not general enough to describe modifications in $(n > 2)$-body Higgs decays resulting in non-SM kinematics. Similarly, the old κ framework could not describe modifications of the Higgs-cross sections that cannot be reabsorbed into a simple overall re-scaling with respect to the SM.

Similarly to the case of electroweak observables, it is convenient to introduce two complementary sets of Higgs PO:

- a set of *physical* PO, namely a set of (idealized) partial decay rates and asymmetries;
- a set of *effective-couplings* PO, parameterizing the on-shell production and decay amplitudes.

The two sets are in one-to-one correspondence: by construction, the effective-couplings PO are directly related to the physical PO after properly working out the decay kinematics. From the practical point of view, in the LHC Higgs analysis, *effective-couplings* PO are first extracted and from these *physical* PO are obtained providing a more intuitive presentation of the measurement as will be discussed below.

2 Two-body decay modes

In the case of two-body Higgs decays into on-shell SM particles, namely $h \to f\bar{f}$ and $h \to \gamma\gamma$, the natural *physical PO* for each mode are the partial decay widths, and possibly the polarization asymmetry if the spin of the final state is accessible.

In the $h \to f\bar{f}$ case the main issue to be addressed is the optimal definition of the partial decay width taking into account the final state QED and QCD radiation.

In the $h \to \gamma\gamma$ case the point to be addressed is the extrapolation to real photons of electromagnetic showers with non-vanishing invariant mass.

2.1 $h \to f\bar{f}$

For each fermion species we can decompose the on-shell $h \to f\bar{f}$ amplitude in terms of two effective couplings ($y^f_{S,P}$), defined by

$$\mathcal{A}(h \to f\bar{f}) = -\frac{i}{\sqrt{2}}\left(y^f_S \bar{f} f + i y^f_P \bar{f}\gamma_5 f\right) \ . \tag{1}$$

These couplings are real in the limit where we neglect re-scattering effects, that is an excellent approximation (also beyond the SM if we assume no new light states), for all the accessible $h \to f\bar{f}$ channels. If h is a CP-even state (as in the SM), then y^f_P is a CP-violating coupling.

In order to match our notation with the κ framework [8], we define the two *effective couplings* PO of the $h \to f\bar{f}$ decays as follows:

$$\kappa_f = \frac{\mathrm{Re}(y^f_S)}{\mathrm{Re}(y^{f,\mathrm{SM}}_S)} \ , \qquad \lambda^{\mathrm{CP}}_f = \frac{\mathrm{Re}(y^f_P)}{\mathrm{Re}(y^{f,\mathrm{SM}}_S)} \ . \tag{2}$$

Here $y^{f,\mathrm{SM}}_S$ is the SM effective coupling that provides the best SM prediction in the $\kappa_f \to 1$ and $\lambda^{\mathrm{CP}}_f \to 0$ limit.

The measurement of $\Gamma(h \to f\bar{f})_{(\rm incl)}$ determines the combination $|\kappa_f|^2 + |\lambda_f^{\rm CP}|^2$, while the $\lambda_f^{\rm CP}/\kappa_f$ ratio can be determined only if the lepton polarization is experimentally accessible. With this notation, the inclusive decay rates, computed assuming a pure bremsstrahlung spectrum can be written as

$$\Gamma(h \to f\bar{f})_{(\rm incl)} = \left[\kappa_f^2 + (\lambda_f^{\rm CP})^2\right] \Gamma(h \to f\bar{f})^{(\rm SM)}_{(\rm incl)} \ , \tag{3}$$

where fermion-mass effects, of per-mil level even for the b quark, have been neglected. In experiments $\Gamma(h \to f\bar{f})_{(\rm incl)}$ cannot be directly accessed, given tight cuts on the $f\bar{f}$ invariant mass to suppress the background: $\Gamma(h \to f\bar{f})_{(\rm incl)}$ is extrapolated from the experimentally accessible $\Gamma(h \to f\bar{f})_{(\rm cut)}$ assuming a pure bremsstrahlung spectrum, both as far as QED and as far as QCD (for the $q\bar{q}$ channels only) radiation is concerned.

The SM decay width is given by

$$\Gamma(h \to f\bar{f})^{(\rm SM)}_{(\rm incl)} = N_c^f \frac{|y_{\rm eff}^{f,\rm SM}|^2}{16\pi} m_H^2 \ , \tag{4}$$

where the color factor N_c^f is 3 for quarks and 1 for leptons. Using the best SM prediction of the branching ratios in these channels [8], for $m_H = 125.0$ GeV and $\Gamma_H^{\rm tot} = 4.07\times10^{-3}$ GeV, we extract the values of the $|y_{\rm eff}^{f,\rm SM}|$ couplings in Eq. (4):

	$\bar{b}b$	$\bar{\tau}\tau$
$\mathcal{B}(h \to \bar{f}f)$	5.77×10^{-1}	6.32×10^{-2}
$\lvert y_{\rm eff}^{f,\rm SM}\rvert$	1.77×10^{-2}	1.02×10^{-2}

,

	$\bar{c}c$	$\bar{\mu}\mu$
$\mathcal{B}(h \to \bar{f}f)$	2.91×10^{-2}	2.19×10^{-4}
$\lvert y_{\rm eff}^{f,\rm SM}\rvert$	3.98×10^{-3}	5.99×10^{-4}

,

As anticipated, the physical PO sensitive to $\lambda_f^{\rm CP}/\kappa_f$ necessarily involve a determination (direct or indirect) of the fermion spins. Denoting by $\vec{k}_f$ the 3-momentum of the fermion f in the Higgs center of mass frame, and with $\{\vec{s}_f, \vec{s}_{\bar{f}}\}$ the two fermion spins, we can define the following CP-odd asymmetry [9]

$$\mathcal{A}_f^{\rm CP} = \frac{1}{|\vec{k}_f|} \langle \vec{k}_f \cdot (\vec{s}_f \times \vec{s}_{\bar{f}}) \rangle = -\frac{\lambda_f^{\rm CP}\kappa_f}{\kappa_f^2 + (\lambda_f^{\rm CP})^2} \tag{5}$$

As pointed out in Ref. [10], in the $h \to \tau^+\tau^- \to X_{\tau^+}X_{\tau^-}$ decay chains asymmetries proportional to $\mathcal{A}_f^{\rm CP}$ are accessible through the measurement of the angular distribution of the $\tau^\pm$ decay products.

Note that, by construction, the effective couplings PO depend on the SM normalization. This imply an intrinsic theoretical uncertainty in their determination related to the theory error on the SM reference value. On the other hand, the physical PO are independent of any reference to the SM. Indeed the (conventional) SM normalization of κ_f cancels in Eq. (3).

2.2 $h \to \gamma\gamma$

The general decomposition for the $h \to \gamma\gamma$ amplitude is

$$\mathcal{A}\left[h \to \gamma(q,\epsilon)\gamma(q',\epsilon')\right] \;=\; i\frac{2}{v_F}\epsilon'_\mu\epsilon_\nu\left[\epsilon_{\gamma\gamma}(g^{\mu\nu}\; q{\cdot}q' - q^\mu q'^\nu) + \epsilon^{\rm CP}_{\gamma\gamma}\varepsilon^{\mu\nu\rho\sigma}q_\rho q'_\sigma\right] \;, \tag{6}$$

from which we identify the two effective couplings $\epsilon_{\gamma\gamma}$ and $\epsilon^{\rm CP}_{\gamma\gamma}$ that, similarly to $y^f_{S,P}$, can be assumed to be real in the limit where we assume no new light states and small deviations from the SM limit. We define the effective couplings PO for this channels as

$$\kappa_{\gamma\gamma} = \frac{{\rm Re}(\epsilon_{\gamma\gamma})}{{\rm Re}(\epsilon^{\rm SM}_{\gamma\gamma})} \;, \qquad \lambda^{\rm CP}_{\gamma\gamma} = \frac{{\rm Re}(\epsilon^{\rm CP}_{\gamma\gamma})}{{\rm Re}(\epsilon^{\rm SM}_{\gamma\gamma})} \;, \tag{7}$$

where $\epsilon^{\gamma\gamma}_{\rm SM}$ is the value of the PO which reproduces the best SM prediction of the decay width. By construction, the SM expectation for the two PO is $\kappa^{\rm SM}_{\gamma\gamma} = 1$ and $(\lambda^{\rm CP}_{\gamma\gamma})^{\rm SM} = 0$.

If the photon polarization is not accessible, the only physical PO for this channel is $\Gamma(h \to \gamma\gamma)$. Starting from realistic observables, where the electromagnetic showers have non-vanishing invariant mass, $\Gamma(h \to \gamma\gamma)$ is defined as the extrapolation to the limit of zero invariant mass for the electromagnetic showers. The relation between $\Gamma(h \to \gamma\gamma)$ and the two effective couplings PO is

$$\Gamma(h \to \gamma\gamma) = \left[\kappa^2_{\gamma\gamma} + (\lambda^{\rm CP}_{\gamma\gamma})^2\right]\Gamma(h \to \gamma\gamma)^{\rm (SM)} \;, \tag{8}$$

where

$$\Gamma(h \to \gamma\gamma)^{\rm (SM)} = \frac{|\epsilon^{\rm SM,eff}_{\gamma\gamma}|^2}{16\pi}\frac{m_H^3}{v_F^2}. \tag{9}$$

Using the SM prediction for the branching ratios in two photons [8], for $v_F = 246.22$ GeV, $m_H = 125.0$ GeV and $\Gamma^{\rm tot}_H = 4.07 \times 10^{-3}$ GeV, we obtain

$$\mathcal{B}(h \to \gamma\gamma)^{\rm SM} = 2.28 \times 10^{-3} \quad \to \quad \epsilon^{\gamma\gamma}_{\rm SM} = 3.8 \times 10^{-3} \;. \tag{10}$$

This value corresponds to the 1-loop contribution in the SM, which also fixes the relative sign. Similarly to the $f\bar{f}$ case, the SM normalization cancels in the definition of the physical PO.

The physical PO linear in the CP-violating coupling $\lambda^{\rm CP}_{\gamma\gamma}$ necessarily involves the measurement of the photon polarization and is therefore hardly accessible at the LHC (at lest in a direct way). Denoting by $\vec{q}_{1,2}$ the 3-momenta of the two photons in the center of mass frame, and with $\vec{\epsilon}_{1,2}$ the corresponding polarization vectors, we can define [to be checked]:

$$\mathcal{A}^{\rm CP}_{\gamma\gamma} = \frac{1}{m_h}\langle(\vec{q}_1 - \vec{q}_2)\cdot(\vec{\epsilon}_1 \times \vec{\epsilon}_2)\rangle = \frac{\lambda^{\rm CP}_{\gamma\gamma}\kappa_{\gamma\gamma}}{\kappa^2_{\gamma\gamma} + (\lambda^{\rm CP}_{\gamma\gamma})^2} \;. \tag{11}$$

3 Three-body decay modes

The guiding principle for the definition of PO in multi-body channels is the decomposition of the decay amplitudes in terms of contributions associated to a specific single-particle pole structure. In the absence of new light states, such poles are generated only by the exchange of the SM electroweak bosons (γ, Z, and W) or by hadronic resonances (whose contribution appears only beyond the tree level and is largely suppressed). Since positions and residues on the poles are gauge-invariant quantities, this decomposition satisfies the general requirements for the definitions of PO.

3.1 $h \to f\bar{f}\gamma$

The general form factor decomposition for these channels is

$$\begin{aligned}\mathcal{A}\left[h \to f(p_1)\bar{f}(p_2)\gamma(q,\epsilon)\right] &= i\frac{2}{v_F}\sum_{f=f_L,f_R}(\bar{f}\gamma_\mu f)\epsilon_\nu \times \\ &\times \left[F_T^{f\gamma}(p^2)(p\cdot q\; g^{\mu\nu} - q^\mu p^\nu) + F_{CP}^{f\gamma}(p^2)\varepsilon^{\mu\nu\rho\sigma}q_\rho p_\sigma\right], \quad (12)\end{aligned}$$

where $p = p_1 + p_2$. The form factors can be further decomposed as

$$F_T^{f\gamma}(p^2) = \epsilon_{Z\gamma}\frac{g_Z^f}{P_Z(p^2)} + \epsilon_{\gamma\gamma}\frac{eQ_f}{p^2} + \Delta_{f\gamma}^{\rm SM}(p^2)\ , \quad (13)$$

$$F_{CP}^{f\gamma}(p^2) = \epsilon_{Z\gamma}^{\rm CP}\frac{g_Z^f}{P_Z(p^2)} + \epsilon_{\gamma\gamma}^{\rm CP}\frac{eQ_f}{p^2}\ . \quad (14)$$

Here g_Z^f are the effective PO describing on-shell $Z \to f\bar{f}$ decays[1] and $P_Z(q^2) = q^2 - m_Z^2 + im_Z\Gamma_Z$. In other words, we decompose the form factors identifying the physical poles associated to the Z and γ propagators.

The term $\Delta_{f\gamma}^{\rm SM}(p^2)$ denotes the remnant of the SM $h \to f\bar{f}\gamma$ loop function that is regular both in the limit $p^2 \to 0$ and in the limit $p^2 \to m_Z^2$. This part of the amplitude is largely subdominant (being not enhanced by a physical single-particle pole) and cannot receive non-standard contributions from operators of dimension up to 6 in the EFT approach to Higgs physics. For this reason it is fixed to its SM value.

In this channel we thus have four effective couplings PO, related to the four ϵ_X terms in Eqs. (13) and (14), two of which are accessible also in $h \to 2\gamma$. Similarly to the $h \to 2\gamma$ case, it is convenient to define the PO normalizing them the corresponding reference SM values of the amplitudes. We thus define

$$\kappa_{Z\gamma} = \frac{\mathrm{Re}(\epsilon_{Z\gamma})}{\mathrm{Re}(\epsilon_{Z\gamma}^{\rm SM})}\ , \qquad \lambda_{Z\gamma}^{\rm CP} = \frac{\mathrm{Re}(\epsilon_{Z\gamma}^{\rm CP})}{\mathrm{Re}(\epsilon_{Z\gamma}^{\rm SM})}\ , \quad (15)$$

[1] We have absorbed a factor $g/\cos(\theta_W)$ with respect to the definition of the effective Z couplings adopted at LEP-1 (and employed in the so-called *Higgs Basis* Lagrangian), see Eq. (24).

where the numerical value of the SM contribution $\epsilon_{Z\gamma}^{\rm SM}$ is obtained from the best SM prediction for the $h \to Z\gamma$ decay width.

The simplest physical PO that can be extracted from this channel is $\Gamma(h \to Z\gamma)$, where both the Z boson and the photon are on-shell. By construction, this can be written as

$$\Gamma(h \to Z\gamma) = \left[\kappa_{Z\gamma}^2 + (\lambda_{Z\gamma}^{\rm CP})^2\right] \Gamma(h \to Z\gamma)^{(\rm SM)} \ , \tag{16}$$

where

$$\Gamma(h \to Z\gamma)^{(\rm SM)} = \frac{|\epsilon_{Z\gamma}^{\rm SM,eff}|^2}{8\pi} \frac{m_H^3}{v^2} \left(1 - \frac{m_Z^2}{m_H^2}\right)^3 \ . \tag{17}$$

The SM prediction for this decay rate [8] provides the value of $\epsilon_{\rm SM}^{Z\gamma}$:

$$\mathcal{B}(h \to Z\gamma)^{(\rm SM)} = 1.54 \times 10^{-3} \quad \to \quad \epsilon_{Z\gamma}^{\rm SM} = 6.9 \times 10^{-3} \ . \tag{18}$$

The independent physical PO linear in the coupling $\lambda_{Z\gamma}^{\rm CP}$ is the following CP-odd asymmetry at the Z peak [to be checked]:

$$\mathcal{A}_{Z\gamma}^{\rm CP} = \frac{1}{|\vec{p}||\vec{q}|} \langle \vec{p} \cdot (\vec{q} \times \vec{\epsilon_\gamma}) \rangle \Big|_{(p^2 = m_Z^2)} = \frac{\lambda_{Z\gamma}^{\rm CP} \kappa_{Z\gamma}}{\kappa_{Z\gamma}^2 + (\lambda_{Z\gamma}^{\rm CP})^2} \ , \tag{19}$$

where all 3-momenta are defined in the Higgs center of mass frame.

This channel is also sensitive to $\Gamma(h \to \gamma\gamma)$ and $\mathcal{A}_{\gamma\gamma}^{\rm CP}$ via the effective couplings $\kappa_{\gamma\gamma}$ (or $\epsilon_{\gamma\gamma}$) and $\lambda_{\gamma\gamma}^{\rm CP}$ (or $\epsilon_{\gamma\gamma}^{\rm CP}$). Determining such couplings from a fit to the from factors in the low p^2 region, one can indirectly determine $\Gamma(h \to \gamma\gamma)$ and $\mathcal{A}_{\gamma\gamma}^{\rm CP}$ by means of Eq. (8) and Eq. (11), respectively.

4 Four-fermion decay modes

Similarly to the three-body modes, also in this case the guiding principle for the definition of PO is the decomposition of the decay amplitudes in terms of contributions associated to a specific pole structure. Such decomposition for the $h \to 4f$ channels has been presented in Ref. [3]. The effective coupling PO that appear in these channels consist of four sets:

- 3 flavor-universal charged-current PO: $\{\kappa_{WW}, \epsilon_{WW}, \epsilon_{WW}^{\rm CP}\}$;
- 7 flavor-universal neutral-current PO, 4 of which are appearing already in $h \to \gamma\gamma$ and $h \to f\bar{f}\gamma$: $\{\kappa_{\gamma\gamma}, \lambda_{\gamma\gamma}^{\rm CP}, \kappa_{Z\gamma}, \lambda_{Z\gamma}^{\rm CP}\}$, and another 3 which are specific for $h \to 4f$: $\{\kappa_{ZZ}, \epsilon_{ZZ}, \epsilon_{ZZ}^{\rm CP}\}$;
- the set of flavor non-universal charged-current PO: $\{\epsilon_{Wf}\}$;
- the set of flavor non-universal neutral-current PO: $\{\epsilon_{Zf}\}$.

While the number of flavor-universal PO is fixed, the number of flavor non-universal PO depend on the fermion species we are interested in. For instance, looking only at light leptons ($\ell = e, \mu$), we have 4 flavor non-universal PO contributing to $h \to 4\ell$ modes (ϵ_{Zf}, with $f = e_L, e_R, \mu_L, \mu_R$) and 4 PO contributing to $h \to 2\ell 2\nu$ modes ($\epsilon_{We_L}, \epsilon_{W\mu_L}, \epsilon_{Z\nu_e}, \epsilon_{Z\nu_\mu}$). The definition of these PO is done at the amplitude level, separating neutral-current and charged-current contributions to the $h \to 4f$ processes, as discussed below.

Starting from each of the effective couplings PO we can define a corresponding physical PO. In particular, $\Gamma(h \to ZZ)$ is defined as the (ideal) rate extracted from the full $\Gamma(h \to 4f)$, extrapolating the result in the limit $\kappa_{ZZ} \neq 0$ and all the other effective couplings set to zero. Similarly $\Gamma(h \to Zf\bar{f})$ is defined from the extrapolation in the limit $\epsilon_{Zf} \neq 0$ and all the other effective couplings set to zero (see extended discussion below).

4.1 $h \to 4f$ neutral currents

Let us consider the case of two different (light) fermion species: $h \to f\bar{f} + f'\bar{f}'$. Neglecting helicity-violating terms (yielding contributions suppressed by light fermion masses in the rates), we can decompose the neutral-current contribution to the amplitude in the following way

$$\begin{aligned}
&\mathcal{A}_{n.c.}\left[h \to f(p_1)\bar{f}(p_2)f'(p_3)\bar{f}'(p_4)\right] = i\frac{2m_Z^2}{v_F}\sum_{f=f_L,f_R}\sum_{f'=f'_L,f'_R}(\bar{f}\gamma_\mu f)(\bar{f}'\gamma_\nu f')\mathcal{T}^{\mu\nu}_{n.c.}(q_1,q_2)\\
&\mathcal{T}^{\mu\nu}_{n.c.}(q_1,q_2) = \left[F_L^{ff'}(q_1^2,q_2^2)g^{\mu\nu} + F_T^{ff'}(q_1^2,q_2^2)\frac{q_1\cdot q_2\; g^{\mu\nu} - q_2{}^\mu q_1{}^\nu}{m_Z^2} + F_{CP}^{ff'}(q_1^2,q_2^2)\frac{\varepsilon^{\mu\nu\rho\sigma}q_{2\rho}q_{1\sigma}}{m_Z^2}\right],
\end{aligned} \tag{20}$$

where $q_1 = p_1 + p_2$ and $q_2 = p_3 + p_4$. The form factor F_L describes the interaction with the longitudinal part of the current, as in the SM, the F_T term describes the interaction with the transverse part, while F_{CP} describes the CP-violating part of the interaction (if the Higgs is assumed to be a CP-even state).

We can further expand the form factors in full generality around the poles, providing

the definition of the neutral-current PO [3]:

$$F_L^{ff'}(q_1^2,q_2^2) = \kappa_{ZZ}\frac{g_Z^f g_Z^{f'}}{P_Z(q_1^2)P_Z(q_2^2)} + \frac{\epsilon_{Zf}}{m_Z^2}\frac{g_Z^{f'}}{P_Z(q_2^2)} + \frac{\epsilon_{Zf'}}{m_Z^2}\frac{g_Z^{f}}{P_Z(q_1^2)} + \Delta_L^{\rm SM}(q_1^2,q_2^2)\ , \quad (21)$$

$$F_T^{ff'}(q_1^2,q_2^2) = \epsilon_{ZZ}\frac{g_Z^f g_Z^{f'}}{P_Z(q_1^2)P_Z(q_2^2)} + \epsilon_{Z\gamma}\left(\frac{eQ_{f'}g_Z^f}{q_2^2P_Z(q_1^2)} + \frac{eQ_f g_Z^{f'}}{q_1^2P_Z(q_2^2)}\right) + \epsilon_{\gamma\gamma}\frac{e^2Q_fQ_{f'}}{q_1^2q_2^2} + \Delta_T^{\rm SM}(q_1^2,q_2^2), \quad (22)$$

$$F_{CP}^{ff'}(q_1^2,q_2^2) = \epsilon_{ZZ}^{\rm CP}\frac{g_Z^f g_Z^{f'}}{P_Z(q_1^2)P_Z(q_2^2)} + \epsilon_{Z\gamma}^{\rm CP}\left(\frac{eQ_{f'}g_Z^f}{q_2^2P_Z(q_1^2)} + \frac{eQ_f g_Z^{f'}}{q_1^2P_Z(q_2^2)}\right) + \epsilon_{\gamma\gamma}^{\rm CP}\frac{e^2Q_fQ_{f'}}{q_1^2q_2^2} \quad (23)$$

Here g_Z^f are Z-pole PO extracted from Z decays at LEP-I, the translation to the notation used at LEP being very simple

$$g_Z^f = \frac{2m_Z}{v_F}g_f^{\rm LEP}\ , \qquad \text{and} \qquad (g_Z^f)_{\rm SM} = \frac{2m_Z}{v_F}(T_3^f - Q_f s^2_{\theta_W})\ . \quad (24)$$

As anticipated, all the parameters but ϵ_{Zf} and g_Z^f are flavor universal, i.e. they do not depend on the fermion species. In fact, flavor non-universal effects in g_Z^f have been very tightly constrained at LEP, however, sizeable effects in ϵ_{Zf} are possible and should be tested at the LHC. In the limit where we neglect re-scattering effects, both κ_{ZZ} and ϵ_X are real. The functions $\Delta_{L,T}^{\rm SM}(q_1^2,q_2^2)$ denote subleading non-local contributions that are regular both in the limit $q_{1,2}^2 \to 0$ and in the limit $q_{1,2}^2 \to m_Z^2$. As in the 3-body decay case, this part of the amplitude is largely subdominant and not affected by operators with dimension up to 6, therefore it is fixed it to its SM value.

4.2 $h \to 4f$ charged currents

Let us consider the $h \to \ell\bar\nu_\ell\bar\ell'\nu_{\ell'}$ process.[2] Employing the same assumptions used in the neutral current case, we can decompose the amplitude in the following way:

$$\mathcal{A}_{c.c.}\left[h \to \ell(p_1)\bar\nu_\ell(p_2)\nu_{\ell'}(p_3)\bar\ell'(p_4)\right] = i\frac{2m_W^2}{v_F}(\bar\ell_L\gamma_\mu\nu_{\ell L})(\bar\nu_{\ell' L}\gamma_\nu\ell'_L)\mathcal{T}_{c.c.}^{\mu\nu}(q_1,q_2)$$
$$\mathcal{T}_{c.c.}^{\mu\nu}(q_1,q_2) = \left[G_L^{\ell\ell'}(q_1^2,q_2^2)g^{\mu\nu} + G_T^{\ell\ell'}(q_1^2,q_2^2)\frac{q_1\cdot q_2\ g^{\mu\nu} - q_2{}^\mu q_1{}^\nu}{m_W^2} + G_{CP}^{\ell\ell'}(q_1^2,q_2^2)\frac{\varepsilon^{\mu\nu\rho\sigma}q_{2\rho}q_{1\sigma}}{m_W^2}\right], \quad (25)$$

[2] The analysis of a process involving quarks is equivalent, with the only difference that the ϵ_{Wf} coefficients are in this case non-diagonal matrices in flavor space, as the g_{ud}^W effective couplings.

where $q_1 = p_1 + p_2$ and $q_2 = p_3 + p_4$. The decomposition of the form factors, that allows us to define the charged-current PO, is [3]

$$G_L^{\ell\ell'}(q_1^2, q_2^2) = \kappa_{WW} \frac{(g_W^\ell)^* g_W^{\ell'}}{P_W(q_1^2) P_W(q_2^2)} + \frac{(\epsilon_{W\ell})^*}{m_W^2} \frac{g_W^{\ell'}}{P_W(q_2^2)} + \frac{\epsilon_{W\ell'}}{m_W^2} \frac{(g_W^\ell)^*}{P_W(q_1^2)} , \tag{26}$$

$$G_T^{\ell\ell'}(q_1^2, q_2^2) = \epsilon_{WW} \frac{(g_W^\ell)^* g_W^{\ell'}}{P_W(q_1^2) P_W(q_2^2)} , \tag{27}$$

$$G_{CP}^{\ell\ell'}(q_1^2, q_2^2) = \epsilon_{WW}^{\rm CP} \frac{(g_W^\ell)^* g_W^{\ell'}}{P_W(q_1^2) P_W(q_2^2)} , \tag{28}$$

where $P_W(q^2)$ is the W propagator defined analogously to $P_Z(q^2)$ and g_W^f are the effective couplings describing on-shell W decays (we have absorbed a factor of g compared to standard notations). In the SM

$$(g_W^{ik})_{\rm SM} = \frac{g}{\sqrt{2}} V_{ik} , \tag{29}$$

where V is the CKM mixing matrix.[3] In absence of rescattering effects, the Hermiticity of the underlying effective Lagrangian implies that κ_{WW}, ϵ_{WW} and $\epsilon_{WW}^{\rm CP}$ are real couplings, while $\epsilon_{W\ell}$ can be complex.

4.3 $h \to 4f$ complete decomposition

The complete decomposition of a generic $h \to 4f$ amplitude is obtained combining neutral- and charged-current contributions depending on the nature of the fermions involved. For instance $h \to 2e2\mu$ and $h \to \ell\bar{\ell}q\bar{q}$ decays are determined by a single neutral current amplitude, while the case of two identical lepton pairs is obtained from Eq. (20) taking into account the proper (anti-)symmetrization of the amplitude:

$$\begin{aligned} \mathcal{A}\left[h \to \ell(p_1)\bar{\ell}(p_2)\ell(p_3)\bar{\ell}(p_4)\right] &= \mathcal{A}_{n.c.}\left[h \to f(p_1)\bar{f}(p_2)f'(p_3)\bar{f}'(p_4)\right]_{f=f'=\ell} \\ &- \mathcal{A}_{n.c.}\left[h \to f(p_1)\bar{f}(p_4)f'(p_3)\bar{f}'(p_2)\right]_{f=f'=\ell} . \end{aligned} \tag{30}$$

The $h \to e^\pm\mu^\mp\nu\bar{\nu}$ decays receive contributions from a single charged-current amplitude, while in the $h \to \ell\bar{\ell}\nu\bar{\nu}$ case we have to sum charged and neutral-current contributions:

$$\begin{aligned} \mathcal{A}\left[h \to \ell(p_1)\bar{\ell}(p_2)\nu(p_3)\bar{\nu}(p_4)\right] &= \mathcal{A}_{n.c.}\left[h \to \ell(p_1)\bar{\ell}(p_2)\nu(p_3)\bar{\nu}(p_4)\right] \\ &- \mathcal{A}_{c.c.}\left[h \to \ell(p_1)\bar{\nu}(p_4)\nu(p_3)\bar{\ell}(p_2)\right] . \end{aligned} \tag{31}$$

[3] More precisely, $(g_W^{ik})_{\rm SM} = \frac{g}{\sqrt{2}} V_{ik}$ if i and k refers to left-handed quarks, otherwise $(g_W^{ik})_{\rm SM} = 0$.

4.4 Physical PO for $h \to 4\ell$

To define the idealised physical PO we start with the quadratic terms for each of the form factors in Eqs. (21-23), and compute their contribution to the double differential decay rate for $h \to e^+e^-\mu^+\mu^-$ (for κ_{ZZ}, ϵ_{ZZ} and $\epsilon^{\rm CP}_{ZZ}$) and for $h \to Z\ell^+\ell^-$ (for the contact terms $\epsilon_{Z\ell}$).

Decay channel $h \to e^+e^-\mu^+\mu^-$

We choose this particular decay channel for the (conventional) definition of the physical PO because it depends on all the PO relevant for $h \to 4\ell$ and because it does not contain interference between the two fermion currents as in Eq. (30). The independent contributions of the three form factors to the decay rate are:

$$\begin{aligned}
\frac{d\Gamma^{\rm LL}}{dm_1 dm_2} &= \frac{\lambda_p \beta_{10}}{2304\pi^5} \frac{m_Z^4 m_h^3}{v_F^2} m_1 m_2 \sum_{f,f'} \left| F_{\rm L}^{ff'} \right|^2 \ , \\
\frac{d\Gamma^{\rm TT}}{dm_1 dm_2} &= \frac{\lambda_p \beta_4}{1152\pi^5} \frac{m_h^3}{v_F^2} m_1^3 m_2^3 \sum_{f,f'} \left| F_{\rm T}^{ff'} \right|^2 \ , \\
\frac{d\Gamma^{\rm CP}}{dm_1 dm_2} &= \frac{\lambda_p \beta_2}{1152\pi^5} \frac{m_h^3}{v_F^2} m_1^3 m_2^3 \sum_{f,f'} \left| F_{\rm CP}^{ff'} \right|^2 \ ,
\end{aligned} \tag{32}$$

where $f = e_L, e_R$, $f' = \mu_L, \mu_R$, $m_{1(2)} \equiv \sqrt{q^2_{1(2)}}$ and

$$\lambda_p = \sqrt{1 + \left(\frac{m_1^2 - m_2^2}{m_h^2} \right)^2 - 2\frac{m_1^2 + m_2^2}{m_h^2}} \ , \qquad \beta_N = 1 + \frac{m_1^4 + N m_1^2 m_2^2 + m_2^4}{m_h^4} - 2\frac{m_1^2 + m_2^2}{m_h^2} \ . \tag{33}$$

Inside the each term of the type $\sum_{f,f'} \left| F_i^{ff'} \right|^2$, we extract only the quadratic terms in each PO. By integrating in m_1 and m_2 we obtain the partial decay rates as given by each PO separately (in the limit where the others are negligible):

$$\begin{aligned}
\Gamma(h \to 2e2\mu)[\kappa_{ZZ}] &= 4.929 \times 10^{-2} (|g_{Ze_L}|^2 + |g_{Ze_R}|^2)(|g_{Z\mu_L}|^2 + |g_{Z\mu_R}|^2) \ |\kappa_{ZZ}|^2 \ \text{MeV} \\
\Gamma(h \to 2e2\mu)[\epsilon_{ZZ}] &= 4.458 \times 10^{-3} (|g_{Ze_L}|^2 + |g_{Ze_R}|^2)(|g_{Z\mu_L}|^2 + |g_{Z\mu_R}|^2) \ |\epsilon_{ZZ}|^2 \ \text{MeV} \\
\Gamma(h \to 2e2\mu)[\epsilon^{\rm CP}_{ZZ}] &= 1.884 \times 10^{-3} (|g_{Ze_L}|^2 + |g_{Ze_R}|^2)(|g_{Z\mu_L}|^2 + |g_{Z\mu_R}|^2) \ |\epsilon^{\rm CP}_{ZZ}|^2 \ \text{MeV}
\end{aligned} \tag{34}$$

The numerical coefficients in Eq. (34) have been obtained neglecting QED corrections. The latter must be included at the simulation level by appropriate QED showering programs, such as PHOTOS [11]. As shown in Ref. [12]: the impact of such corrections is negligible after integrating over the full phase space, hence in the overall normalization

of the partial rates in Eq. (34), while they can provide sizable distortions of the spectra in specific phase-space regions.

Since each effective coupling PO correspond to a well-defined pole contribution to the amplitude (with one or two poles of the Z boson), and a well-defined Lorentz and flavor structure, we can associate to the those partial rates a well-defined physical meaning. In particular, we define the following *physical PO* for the $h \to 4\ell$ decays:

$$\begin{aligned}
\Gamma(h \to Z_L Z_L) &\equiv \frac{\Gamma(h \to 2e2\mu)[\kappa_{ZZ}]}{\mathcal{B}(Z \to 2e)\mathcal{B}(Z \to 2\mu)} = 0.209\ |\kappa_{ZZ}|^2\ \text{MeV} \\
\Gamma(h \to Z_T Z_T) &\equiv \frac{\Gamma(h \to 2e2\mu)[\epsilon_{ZZ}]}{\mathcal{B}(Z \to 2e)\mathcal{B}(Z \to 2\mu)} = 0.0189\ |\epsilon_{ZZ}|^2\ \text{MeV} \\
\Gamma^{\text{CPV}}(h \to Z_T Z_T) &\equiv \frac{\Gamma(h \to 2e2\mu)[\epsilon^{\text{CP}}_{ZZ}]}{\mathcal{B}(Z \to 2e)\mathcal{B}(Z \to 2\mu)} = 0.00799\ |\epsilon^{\text{CP}}_{ZZ}|^2\ \text{MeV}
\end{aligned} \tag{35}$$

where, due to the double pole structure of the amplitude, we have removed the (physical) branching ratios of the $Z \to e^+e^-$ and $Z \to \mu^+\mu^-$ decays. Here

$$\mathcal{B}(Z \to 2\ell) = \frac{\Gamma_0}{\Gamma_Z} R^\ell \left((g_Z^{\ell_L})^2 + (g_Z^{\ell_R})^2 \right) \simeq 0.4856 \left((g_Z^{\ell_L})^2 + (g_Z^{\ell_R})^2 \right) \ , \tag{36}$$

where $\Gamma_0 = \frac{m_Z}{24\pi}$, Γ_Z is the total decay width and $R^\ell = \left(1 + \frac{3}{4\pi}\alpha(m_Z)\right)$ describes final state QED radiation.

Decay channel $h \to Z\ell^+\ell^-$

The idealised physical PO related to the contact terms can be defined directly from the on-shell decay $h \to Z\ell^+\ell^-$, where $\ell = e_L, e_R, \mu_L, \mu_R$ and the Z boson is assumed to be on-shell (narrow width approximation). We compute this decay rate, neglecting QED corrections and light lepton masses, in presence of the contact terms $\epsilon_{Z\ell}$ only. The Dalitz double differential rate in $s_{12} \equiv (p_{\ell^+} + p_{\ell^-})^2$ and $s_{23} \equiv (p_{\ell^-} + p_Z)^2$ is

$$\frac{d\Gamma}{ds_{12}ds_{23}} = \frac{1}{(2\pi)^3} \frac{1}{32m_h^2} \frac{4|\epsilon_{Z\ell}|^2}{v^2} \left(s_{12} + \frac{(s_{23} - m_Z^2)(m_h^2 - s_{12} - s_{23})}{m_Z^2} \right) \ , \tag{37}$$

The allowed kinematical region is $0 < s_{12} < (m_h - m_Z)^2$ and, for any given value of s_{12}, $s_{23}^{\text{min}} < s_{23} < s_{23}^{\text{Max}}$ with

$$s_{23}^{\text{min(Max)}} = (E_2^* + E_Z^*)^2 - \left(E_2^* \pm \sqrt{(E_Z^*)^2 - m_Z^2} \right)^2 \ , \tag{38}$$

where $E_2^* = \sqrt{s_{12}}/2$ and $E_Z^* = \frac{m_h^2 - s_{12} - m_Z^2}{2\sqrt{s_{12}}}$. The total decay width defines the relation between the physical PO and the effective couplings PO as:

$$\Gamma(h \to Z\ell^+\ell^-) = 0.0366 |\epsilon_{Z\ell}|^2\ \text{MeV} \ . \tag{39}$$

Together with the physical PO already defined for $h \to \gamma\gamma$ and $h \to Z\gamma$, we have thus established a complete mapping between the effective couplings PO and the physical PO appearing in $h \to 4\ell$ decays.

4.5 Physical PO for $h \to 2\ell 2\nu$

Physical observables for charged-current processes can be defined in a very similar way as the neutral-current ones. In particular, we use the $h \to e^+\nu_e\mu^-\bar{\nu}_\mu$ process for the physical PO corresponding to k_{WW}, ϵ_{WW}, and $\epsilon^{\rm CP}_{WW}$, and $h \to W^+\ell\bar{\nu}_\ell$ for the contact terms.

Decay channel $h \to e^+\nu_e\mu^-\bar{\nu}_\mu$

Integrating the differential distributions analogous to Eq. (32) we obtain the expression of the total decay rate in this channel, in the limit where only one PO is turned on:

$$\begin{aligned}
\Gamma(h \to e\mu 2\nu)[\kappa_{WW}] &= 2.20 \times 10^{-4} |g_{We_L}|^2 |g_{W\mu_L}|^2 \, |\kappa_{WW}|^2 \text{ MeV} \\
\Gamma(h \to e\mu 2\nu)[\epsilon_{WW}] &= 4.27 \times 10^{-5} |g_{We_L}|^2 |g_{W\mu_L}|^2 \, |\epsilon_{WW}|^2 \text{ MeV} \\
\Gamma(h \to e\mu 2\nu)[\epsilon^{\rm CP}_{WW}] &= 1.77 \times 10^{-5} |g_{We_L}|^2 |g_{W\mu_L}|^2 \, |\epsilon^{\rm CP}_{WW}|^2 \text{ MeV}
\end{aligned} \tag{40}$$

As in the neutral channel, the *physical PO* are defined from these quantities by factorizing the W branching ratios:

$$\begin{aligned}
\Gamma(h \to W_L W_L) &\equiv \frac{\Gamma(h \to e\mu 2\nu)[\kappa_{WW}]}{\mathcal{B}(W \to e\bar{\nu}_e)\mathcal{B}(W \to \mu\bar{\nu}_\mu)} = 0.841 \, |\kappa_{WW}|^2 \text{ MeV} \\
\Gamma(h \to W_T W_T) &\equiv \frac{\Gamma(h \to e\mu 2\nu)[\epsilon_{WW}]}{\mathcal{B}(W \to e\bar{\nu}_e)\mathcal{B}(W \to \mu\bar{\nu}_\mu)} = 0.163 \, |\epsilon_{WW}|^2 \text{ MeV} \\
\Gamma^{\rm CPV}(h \to W_T W_T) &\equiv \frac{\Gamma(h \to e\mu 2\nu)[\epsilon^{\rm CP}_{WW}]}{\mathcal{B}(W \to e\bar{\nu}_e)\mathcal{B}(W \to \mu\bar{\nu}_\mu)} = 0.0677 \, |\epsilon^{\rm CP}_{WW}|^2 \text{ MeV} \, .
\end{aligned} \tag{41}$$

The W branching ratios are given by

$$\mathcal{B}(W \to \ell\bar{\nu}_\ell) = \frac{\Gamma_0}{\Gamma_W}(g_{W\ell_L})^2 \simeq 0.511 (g_{W\ell_L})^2 \, , \tag{42}$$

where $\Gamma_0 = \frac{m_W}{24\pi}$, Γ_W is the total decay width.

Decay channel $h \to W^+\ell\bar{\nu}_\ell$

Also in this case the physical PO corresponding to the charged-current contact terms are defined in complete analogy to the neutral-current case, starting from the 3-body decay $h \to W^+\ell\bar{\nu}_\ell$. The total decay width computed in the limit where only the contact term PO is switched on defines the relation between the physical PO and the effective couplings PO as:

$$\Gamma(h \to W^+\ell\bar{\nu}_\ell) = 0.143 |\epsilon_{W\ell}|^2 \text{ MeV} \, . \tag{43}$$

PO	Physical PO	Relation to the eff. coupl.
$\kappa_f,\ \lambda_f^{\rm CP}$	$\Gamma(h\to f\bar f)$	$=\ \Gamma(h\to f\bar f)^{(\rm SM)}[(\kappa_f)^2+(\lambda_f^{\rm CP})^2]$
$\kappa_{\gamma\gamma},\ \lambda_{\gamma\gamma}^{\rm CP}$	$\Gamma(h\to\gamma\gamma)$	$=\ \Gamma(h\to\gamma\gamma)^{(\rm SM)}[(\kappa_{\gamma\gamma})^2+(\lambda_{\gamma\gamma}^{\rm CP})^2]$
$\kappa_{Z\gamma},\ \lambda_{Z\gamma}^{\rm CP}$	$\Gamma(h\to Z\gamma)$	$=\ \Gamma(h\to Z\gamma)^{(\rm SM)}[(\kappa_{Z\gamma})^2+(\lambda_{Z\gamma}^{\rm CP})^2]$
κ_{ZZ}	$\Gamma(h\to Z_LZ_L)$	$=\ (0.209\ \text{MeV})\times\lvert\kappa_{ZZ}\rvert^2$
ϵ_{ZZ}	$\Gamma(h\to Z_TZ_T)$	$=\ (1.9\times10^{-2}\ \text{MeV})\times\lvert\epsilon_{ZZ}\rvert^2$
$\epsilon_{ZZ}^{\rm CP}$	$\Gamma^{\rm CPV}(h\to Z_TZ_T)$	$=\ (8.0\times10^{-3}\ \text{MeV})\times\lvert\epsilon_{ZZ}^{\rm CP}\rvert^2$
ϵ_{Zf}	$\Gamma(h\to Zf\bar f)$	$=\ (3.7\times10^{-2}\ \text{MeV})\times N_c^f\ \lvert\epsilon_{Zf}\rvert^2$
κ_{WW}	$\Gamma(h\to W_LW_L)$	$=\ (0.84\ \text{MeV})\times\lvert\kappa_{WW}\rvert^2$
ϵ_{WW}	$\Gamma(h\to W_TW_T)$	$=\ (0.16\ \text{MeV})\times\lvert\epsilon_{WW}\rvert^2$
$\epsilon_{WW}^{\rm CP}$	$\Gamma^{\rm CPV}(h\to W_TW_T)$	$=\ (6.8\times10^{-2}\ \text{MeV})\times\lvert\epsilon_{WW}^{\rm CP}\rvert^2$
ϵ_{Wf}	$\Gamma(h\to Wf\bar f')$	$=\ (0.14\ \text{MeV})\times N_c^f\ \lvert\epsilon_{Wf}\rvert^2$

Table 1: Summary of the *effective coupling* PO and the corresponding *physical* PO. The parameter N_c^f is 1 for leptons and 3 for quarks. In the case of the charged-current contact term, f' is the $SU(2)_L$ partner of the fermion f.

5 PO in Higgs electroweak production: generalities

The PO decomposition of $h\to 4f$ amplitude discussed above can naturally be generalized to describe electroweak Higgs-production processes, namely Higgs-production via vector-boson fusion (VBF) and Higgs-production in association with a massive SM gauge boson (VH).

The interest of such production processes is twofold. On the one hand, they are closely connected to the $h\to 4\ell, 2\ell2\nu$ decay processes by crossing symmetry, and by the exchange of lepton currents into quark currents. As a result, some of the Higgs PO necessary to describe the $h\to 4\ell, 2\ell2\nu$ decay kinematics appear also in the description of the VBF and VH cross sections (independently of the Higgs decay mode). This facts opens the possibility of combined analyses of production cross sections and differential decay distributions, with a significant reduction on the experimental error on the extraction of the PO. On the other hand, the production cross sections allow to explore different kinematical regimes compared to the decays. By construction, the momentum transfer appearing in the Higgs decay amplitudes is limited by the Higgs mass, while such limitation is not present in the production amplitudes. The higher energies probed in the production processes provide an increased sensitivity to new physics effects. This fact also allows to test the momentum expansion that is intrinsic in the PO decomposition, as well as in any effective field theory approach to physics beyond the SM.

Despite the similarities at the fundamental level, the phenomenological description of VBF and VH in terms of PO is significantly more challenging compared to that of Higgs decays. On the one hand, QCD corrections plays a non-negligible role in the production processes. Although technically challenging, this fact does not represent a conceptual problem for the PO approach: the leading QCD corrections factorize in VBF and VH, similarly to the factorization of QED corrections in $h \to 4\ell$. This implies that NLO QCD corrections can be incorporated in general terms with suitable modifications of the existing Montecarlo tools. On the other hand, the relation between the kinematical variables at the basis of the PO decomposition (i.e. the momentum transfer of the partonic currents, q^2) and the kinematical variables accessible in pp collisions is not straightforward, especially in the VBF case. This problem finds a natural solution in the VBF case due to strong correlation between q^2 and the p_T of the VBF tagged jets.

5.1 Amplitude decomposition

Neglecting the light fermion masses, the electroweak production processes VH and VBF or, more precisely, the electroweak partonic amplitudes $f_1 f_2 \to h + f_3 f_4$, can be completely described by the three-point correlation function of the Higgs boson and two (color-less) fermion currents

$$\langle 0|\mathcal{T}\left\{J_f^\mu(x), J_{f'}^\nu(y), h(0)\right\}|0\rangle \ , \tag{44}$$

where all the states involved are on-shell. The same correlation function controls also the four-fermion Higgs decays discussed above. In the $h \to 4\ell, 2\ell 2\nu$ case both currents are leptonic and all fermions are in the final state. In case of VH associate production one of the currents describes the initial state quarks, while the other describes the decay products of the (nearly on-shell) vector boson. Finally, in VBF production the currents are not in the s-channel as in the previous cases, but in the t-channel. Strictly speaking, in VH and VBF the quark states are not on-shell; however, their off-shellness of order $\Lambda_{\rm QCD}$ can be safely neglected compared to the electroweak scale characterizing the process (both within and beyond the SM).

As in the $h \to 4f$ case, we can expand the correlation function in Eq. (44) around the known physical poles due to the propagation of intermediate SM electroweak gauge bosons. The PO are then defined by the residues on the poles and by the non-resonant terms in this expansion. By construction, terms corresponding to a double pole structure are independent from the nature of the fermion current involved. As a result, the corresponding PO are universal and can be extracted from any of the above mention processes, both in production and in decays [7].

5.1.1 Vector boson fusion Higgs production

Higgs production via vector boson fusion (VBF) receives contribution both from neutral- and charged-current channels. Also, depending on the specific partonic process, there

could be two different ways to construct the two currents, and these two terms interfere with each other. For example, for $uu \to uuh$ one has the interference between two neutral-current processes, while in $ud \to udh$ the interference is between neutral and charged currents. In this case it is clear that one should sum the two amplitudes with the proper symmetrization, as done in the case of $h \to 4e$.

We now proceed describing how each of these amplitudes can be parametrized in terms of PO. Let us start with the neutral-current one. The amplitude for the on-shell process $q_i(p_1)q_j(p_2) \to q_i(p_3)q_j(p_4)h(k)$ can be parametrized by

$$\mathcal{A}_{n.c}(q_i(p_1)q_j(p_2) \to q_i(p_3)q_j(p_4)h(k)) = i\frac{2m_Z^2}{v}\bar{q}_i(p_3)\gamma_\mu q_i(p_1)\bar{q}_j(p_4)\gamma_\nu q_j(p_2)\mathcal{T}^{\mu\nu}_{n.c.}(q_1,q_2), \tag{45}$$

where $q_1 = p_1 - p_3$, $q_2 = p_2 - p_4$ and $\mathcal{T}^{\mu\nu}_{n.c.}(q_1,q_2)$ is the same tensor structure appearing in $h \to 4f$ decays. Indeed, proceeding as in Eq. (20), using Lorentz invariance we decompose this tensor structure in term of three from factors:

$$\mathcal{T}^{\mu\nu}_{n.c.}(q_1,q_2) = \left[F_L^{q_iq_j}(q_1^2,q_2^2)g^{\mu\nu} + F_T^{q_iq_j}(q_1^2,q_2^2)\frac{q_1{\cdot}q_2\ g^{\mu\nu} - {q_2}^\mu {q_1}^\nu}{m_Z^2} + F_{CP}^{q_iq_j}(q_1^2,q_2^2)\frac{\varepsilon^{\mu\nu\rho\sigma}q_{2\rho}q_{1\sigma}}{m_Z^2}\right]. \tag{46}$$

Similarly, the charged-current contribution to the amplitude for the on-shell process $u_i(p_1)d_j(p_2) \to d_k(p_3)u_l(p_4)h(k)$ can be parametrized by

$$\mathcal{A}_{c.c}(u_i(p_1)d_j(p_2) \to d_k(p_3)u_l(p_4)h(k)) = i\frac{2m_W^2}{v}\bar{d}_k(p_3)\gamma_\mu u_i(p_1)\bar{u}_l(p_4)\gamma_\nu d_j(p_2)\mathcal{T}^{\mu\nu}_{c.c.}(q_1,q_2), \tag{47}$$

where, again, $\mathcal{T}^{\mu\nu}_{c.c.}(q_1,q_2)$ is the same tensor structure appearing in the charged-current $h \to 4f$ decays:

$$\mathcal{T}^{\mu\nu}_{c.c.}(q_1,q_2) = \left[G_L^{ijkl}(q_1^2,q_2^2)g^{\mu\nu} + G_T^{ijkl}(q_1^2,q_2^2)\frac{q_1{\cdot}q_2\ g^{\mu\nu} - {q_2}^\mu {q_1}^\nu}{m_W^2} + G_{CP}^{ijkl}(q_1^2,q_2^2)\frac{\varepsilon^{\mu\nu\rho\sigma}q_{2\rho}q_{1\sigma}}{m_W^2}\right] \tag{48}$$

The amplitudes for the processes with initial anti-quarks can easily be obtained from the above ones.

The next step is to perform a momentum expansion of the form factors around the physical poles due to the propagation of SM electroweak gauge bosons (γ, Z and $W^\pm$), and to define the PO (i.e. the set $\{\kappa_i, \epsilon_i\}$) from the residues of such poles. We stop this expansion neglecting terms which can be generated only by local operators with dimension higher than six. A discussion about limitations and consistency checks of this procedure will be presented later on. The decomposition of the form factors closely follows the procedure already introduced for the decay amplitudes and will not be repeated here. We report explicitly only expression of the longitudinal form factors, where the contact terms

not accessible in the leptonic decays appear:

$$
\begin{aligned}
F_L^{q_i q_j}(q_1^2, q_2^2) &= \kappa_{ZZ} \frac{g_Z^{q_i} g_Z^{q_j}}{P_Z(q_1^2) P_Z(q_2^2)} + \frac{\epsilon_{Z q_i}}{m_Z^2} \frac{g_Z^{q_j}}{P_Z(q_2^2)} + \frac{\epsilon_{Z q_j}}{m_Z^2} \frac{g_Z^{q_i}}{P_Z(q_1^2)} + \Delta^{\rm SM}_{L,n.c.}(q_1^2, q_2^2) \ , \\
G_L^{ijkl}(q_1^2, q_2^2) &= \kappa_{WW} \frac{g_W^{ik} g_W^{jl}}{P_W(q_1^2) P_W(q_2^2)} + \frac{\epsilon_{W ik}}{m_W^2} \frac{g_W^{jl}}{P_W(q_2^2)} + \frac{\epsilon_{W jl}}{m_W^2} \frac{g_W^{ik}}{P_W(q_1^2)} + \Delta^{\rm SM}_{L,c.c}(q_1^2, q_2^2) \ .
\end{aligned}
\tag{49}
$$

Here $P_V(q^2) = q^2 - m_V^2 + i m_V \Gamma_V$, while g_Z^f and g_W^{ik} are the PO characterizing the on-shell couplings of Z and W boson to a pair of fermions, see eqs.(24) and (29). ~~: within the SM $g_Z^f = \frac{g}{c_{\theta_W}}(T_3^f - Q_f s^2_{\theta_W})$ and $g_W^{ik} = \frac{g}{\sqrt{2}} V_{ik}$, where V is the CKM mixing matrix.~~ The functions $\Delta^{\rm SM}_{L,n.c.(c.c.)}(q_1^2, q_2^2)$ denote non-local contributions generated at the one-loop level (and encoding multi-particle cuts) that cannot be re-absorbed in the definition of κ_i and ϵ_i. At the level of precision we are working, taking into account also the high-luminosity phase of the LHC, these contributions can be safely fixed to their SM values.

As anticipated, the crossing symmetry between $h \to 4f$ and $2f \to h\,2f$ amplitudes ensures that the PO are the same in production and decay (if the same fermions species are involved). The amplitudes are explored in different kinematical regimes in the two type of processes (in particular the momentum-transfers, $q^2_{1,2}$, are space-like in VBF and time-like in $h \to 4f$). However, this does not affect the definition of the PO. This implies that the fermion-independent PO associated to a double pole structure, such as κ_{ZZ} and κ_{WW} in Eq. (49), are expected to be measured with higher accuracy in $h \to 4\ell$ and $h \to 2\ell 2\nu$ rather than in VBF. On the contrary, VBF is particularly useful to constrain the fermion-dependent contact terms $\epsilon_{Z q_i}$ and $\epsilon_{W u_i d_j}$, that appear only in the longitudinal form factors.

5.1.2 Associated vector boson plus Higgs production

The VH production process denote the production of a Higgs boson with a nearly on-shell massive vector boson (W or Z). For simplicity, in the following we will assume that the vector boson is on-shell and that the interference with the VBF amplitude can be neglected. However, we stress that the PO formalism clearly allow to describe both these effects (off-shell V and interference with VBF in case of $V \to \bar{q}q$ decay) simply applying the general decomposition of neutral- and charged-current amplitudes as outlined above.

Similarly to VBF, Lorentz invariance allows us to decompose the amplitudes for the on-shell processes $q_i(p_1)\bar{q}_i(p_2) \to h(p)Z(k)$ and $u_i(p_1)\bar{d}_j(p_2) \to h(p)W^+(k)$ in three possible tensor structures: a longitudinal one, a transverse one, and a CP-odd one,

$$
\begin{aligned}
\mathcal{A}(q_i(p_1)\bar{q}_i(p_2) \to h(p)Z(k)) &= i\frac{2m_Z^2}{v} \bar{q}_i(p_2)\gamma_\nu q_i(p_1) \epsilon_\mu^{Z*}(k) \times \\
&\times \left[F_L^{q_i Z}(q^2) g^{\mu\nu} + F_T^{q_i Z}(q^2) \frac{-(q\cdot k) g^{\mu\nu} + q^\mu k^\nu}{m_Z^2} + F_{CP}^{q_i Z}(q^2) \frac{\epsilon^{\mu\nu\alpha\beta} q_\alpha k_\beta}{m_Z^2} \right] \ ,
\end{aligned}
\tag{50}
$$

$$\mathcal{A}(u_i(p_1)\bar{d}_j(p_2)\to h(p)W^+(k)) = i\frac{2m_W^2}{v}\bar{d}_j(p_2)\gamma_\nu u_i(p_1)\epsilon_\mu^{W*}(k)\times$$
$$\times\left[G_L^{q_{ij}W}(q^2)g^{\mu\nu}+G_T^{q_{ij}W}(q^2)\frac{-(q\cdot k)g^{\mu\nu}+q^\mu k^\nu}{m_W^2}+G_{CP}^{q_{ij}W}(q^2)\frac{\epsilon^{\mu\nu\alpha\beta}q_\alpha k_\beta}{m_W^2}\right], \tag{51}$$

where $q = p_1 + p_2 = k + p$. In the limit where we neglect the off-shellness of the final-sate V, the form factors can only depend on q^2. Already from this decomposition of the amplitude it is clear the importance of providing measurements of the differential cross-section as a function of q^2, as well as differential measurements in terms of the angular variables that allow to disentangle the different tensor structures.

Performing the momentum expansion of the form factors around the physical poles, and defining the PO as in Higgs decays and VBF, we find

$$\begin{aligned}
F_L^{q_iZ}(q^2) &= \kappa_{ZZ}\tfrac{g_{Zq_i}}{P_Z(q^2)}+\tfrac{\epsilon_{Zq_i}}{m_Z^2} & G_L^{q_{ij}W}(q^2) &= \kappa_{WW}\tfrac{(g_W^{u_id_j})^*}{P_W(q^2)}+\tfrac{\epsilon^*_{Wu_id_j}}{m_W^2}\\
F_T^{q_iZ}(q^2) &= \epsilon_{ZZ}\tfrac{g_{Zq_i}}{P_Z(q^2)}+\epsilon_{Z\gamma}\tfrac{eQ_q}{q^2} & G_T^{q_{ij}W}(q^2) &= \epsilon_{WW}\tfrac{(g_W^{u_id_j})^*}{P_W(q^2)}\\
F_{CP}^{q_iZ}(q^2) &= \epsilon_{ZZ}^{\rm CP}\tfrac{g_{Zq_i}}{P_Z(q^2)}-\epsilon_{Z\gamma}^{\rm CP}\tfrac{eQ_q}{q^2} & G_{CP}^{q_{ij}W}(q^2) &= \epsilon_{WW}^{\rm CP}\tfrac{(g_W^{u_id_j})^*}{P_W(q^2)}
\end{aligned} \tag{52}$$

where we have omitted the indication of the (tiny) non-local terms, fixed to their corresponding SM values. As in the VBF case, only the longitudinal form factors F_L and G_L contains PO not accessible in decays, namely the quark contact terms ϵ_{Zq_i} and $\epsilon_{Wu_id_j}$.

6 PO in Higgs electroweak production: phenomenology

6.1 Vector Boson Fusion

At the parton level (i.e. in the $qq \to hqq$ hard scattering) the ideal observable relevant to extract the momentum dependence of the factor factors would be the double differential cross section $d^2\sigma/dq_1^2dq_2^2$, where $q_1 = p_1 - p_3$ and $q_2 = p_2 - p_4$ are the momenta of the two fermion currents entering the process (here p_1, p_2 (p_3, p_4) are the momenta of the initial (final) state quarks). The q_i^2 are also the key variables to test and control the momentum expansion at the basis of the PO decomposition.

A fist nontrivial task is to choose the proper pairing of the incoming and outgoing quarks, given we are experimentally blind to their flavor. For partonic processes receiving two interfering contributions when the final-state quarks are exchanged, such as $uu \to huu$ or $ud \to hud$, the definition of $q_{1,2}$ is even less transparent since a univocal pairing of the momenta can not be assigned, in general, even if one knew the flavor of all partons. This problem can be simply overcome at a practical level by making use of the VBF kinematics, in particular the fact that the two jets are always very forward. This implies one can always pair the momenta of the jet going, for example, on the $+z$ direction with

the initial parton going in the same direction, and viceversa. The same argument can be used to argue that the interference between different amplitudes (e.g. neutral current and charged current) is negligible in VBF. In order to check this, we have performed a leading order parton level simulation of the VBF Higgs production ($pp \to hjj$) using MadGraph5_aMC@NLO [13] (version 2.2.3) at 13 TeV c.m. energy. We have imposed the basic set of cuts,

$$p_{\mathrm{T,j_{1,2}}} > 30 \text{ GeV}, \quad |\eta_{\mathrm{j_{1,2}}}| < 4.5, \quad \text{and} \quad m_{\mathrm{j_1 j_2}} > 500 \text{ GeV}. \tag{53}$$

In Fig. 1, we show the distribution in the opening angle of the incoming and outgoing quark momenta for the two different pairings. The left plot is for the SM, while the right plot is for a specific NP benchmark point. Shown in blue is the pairing based on the leading color connection using the color flow variable while in red is the opposite pairing. The plot shows that the momenta of the color connected quarks tend to form a small opening angle and the overlap between the two curves, i.e. where the interference effects might be sizable, is negligible. This implies that in the experimental analysis the pairing should be done based on this variable. Importantly, the same conclusions can be drawn in the presence of new physics contributions to the contact terms.

There is a potential caveat to the above argument: the color flow approximation ignores the interference terms that are higher order in $1/N_C$. Let us consider a process with two interfering amplitudes with the final state quarks exchanged, for example in $uu \to uuh$. The differential cross section receives three contributions proportional to $|F_L^{ff'}(t_{13}, t_{24})|^2$, $|F_L^{ff'}(t_{13}, t_{24}) F_L^{ff'}(t_{14}, t_{23})|$ and $|F_L^{ff'}(t_{14}, t_{23})|^2$, where $t_{ij} = (p_i - p_j)^2 = -2E_i E_j (1 - \cos\theta_{ij})$. For the validity of the momentum expansion it is important that the momentum transfers (t_{ij}) remain smaller than the hypothesized scale of new physics. On the other hand, imposing the VBF cuts, the interference terms turns out to depend on one small and one large momentum transfer. However, thanks to the pole structure of the form factors, these interference effects turns out to give a very small contribution. Therefore, we can safely state that the momentum transfers marked with the leading color flow are reliable control variables of the momentum expansion validity.

In some realistic experimental analyses, after reconstructing the momenta of the two VBF tagged jets and the Higgs boson, one can compute the relevant momentum transfers q_1 and q_2, adopting the pairing based on the opening angle. However, for some interesting Higgs decays modes, such as $h \to 2\ell 2\nu$, it is not possible to reconstruct the Higgs boson momentum. In this case, a good approximation of the momentum transfer is the jet p_T. This can be understood by explicitly computing the momentum transfer $q^2_{1,2}$ in the limit $|p_T| \ll E_{jet}$ and for a Higgs produced close to threshold. Let us consider the partonic momenta in c.o.m. frame for the process: $p_1 = (E, \vec{0}, E)$, $p_2 = (E, \vec{0}, -E)$, $p_3 = (E'_1, \vec{p}_{T1}, \sqrt{E'^2_1 - p^2_{T1}})$ and $p_4 = (E'_2, \vec{p}_{T2}, \sqrt{E'^2_2 - p^2_{T2}})$. Conservation of energy for the whole process dictates $2E = E'_1 + E'_2 + E_h$, where E^2_h is the Higgs energy, usually of order m_h if the Higgs is not strongly boosted. In this case $E - E'_i = \Delta E_i \ll E$ since the process is symmetric for $1 \leftrightarrow 2$. For each leg, energy and momentum conservation (along

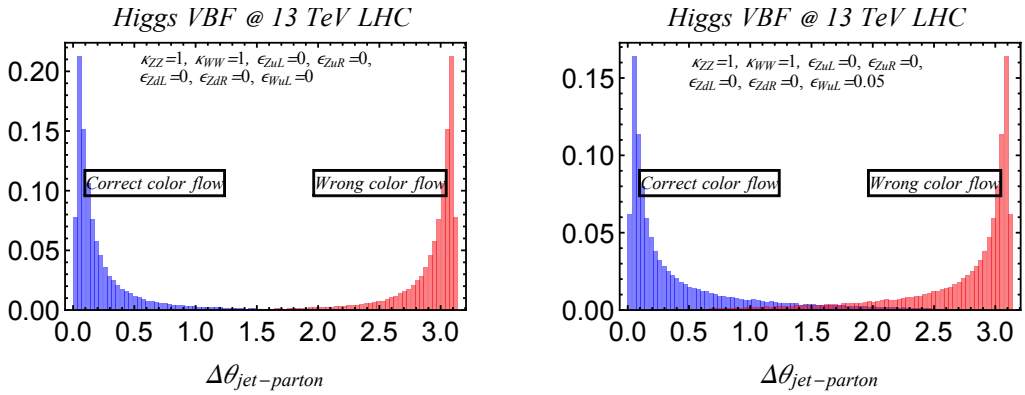

Figure 1: Leading order parton level simulation of the Higgs VBF production at 13 TeV pp c.m. energy. Show in blue is the distribution in the opening angle of the color connected incoming and outgoing quarks $\measuredangle(\vec{p}_3, \vec{p}_1)$, while in red is the distribution for the opposite pairing, $\measuredangle(\vec{p}_3, \vec{p}_2)$. The left plot is for the SM, while the plot on the right is for a specific NP benchmark.

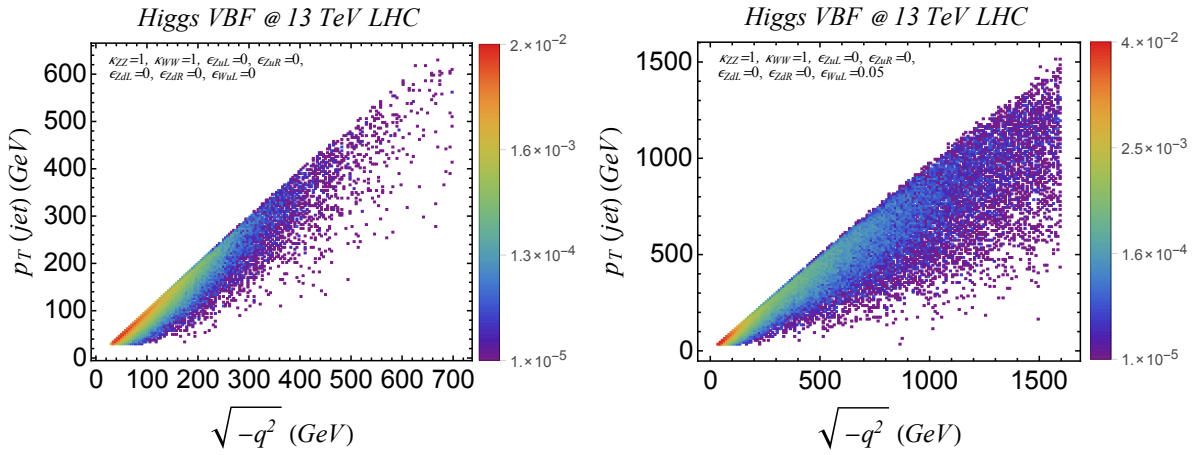

Figure 2: Leading order parton level simulation of the Higgs VBF production at 13 TeV pp c.m. energy. Shown here is the density histogram in two variables; the outgoing quark p_T and the momentum transfer $\sqrt{-q^2}$ with the initial "color-connected" quark. The left plot is for the SM, while the plot on the right is for a specific NP benchmark.

the z axis) give

$$\begin{cases} q_i^z = E - \sqrt{E_i'^2 - p_{Ti}^2} \\ q_i^0 = E - E_i' \end{cases} \quad \to \quad \begin{cases} q_i^0 - q_i^z = \sqrt{E_i'^2 - p_{Ti}^2} - E_i' \approx -\frac{p_{Ti}^2}{2E_i'} \\ q_i^0 + q_i^z \approx 2\Delta E_i + \frac{p_{Ti}^2}{2E_i'} \end{cases} . \tag{54}$$

Putting together these two relations one gets

$$q_i^2 = (q_i^0)^2 - p_{Ti}^2 - (q_i^z)^2 = -p_{Ti}^2 + (q_i^0 - q_i^z)(q_i^0 + q_i^z) \approx -p_{Ti}^2 - \frac{p_{Ti}^2 \Delta E_i}{2E_i'} + \mathcal{O}(p_{Ti}^4/E'^2) . \tag{55}$$

We can thus conclude that, for a Higgs produced near threshold ($\Delta E_i \ll E'$), $q^2 \approx -p_T^2$.

To illustrate the above conclusion, in Fig. 2 we show a density histogram in two variables: the outgoing quark p_T and the momentum transfer $\sqrt{-q^2}$ obtained from the correct color flow pairing (the left and the right plots are for the SM and for a specific NP benchmark, respectively). The plots indicate the strong correlation of the jet p_T with the momentum transfer $\sqrt{-q^2}$ associated with the correct color pairing. We stress that this conclusion holds both within and beyond the SM.

Given the strong $q^2 \leftrightarrow p_T^2$ correlation, we strongly encourage the experimental collaborations to report the unfolded measurement of the double differential distributions in the two VBF tagged jet p_T's: $\tilde{F}(p_{Tj_1}, p_{Tj_2})$. This measurable distribution is closely related to the form factor entering the amplitude decomposition, $F_L(q_1^2, q_2^2)$, and encode (in a model-independent way) the dynamical information about the high-energy behavior of the process. Moreover, the extraction of the PO in VBF must be done preserving the validity of the momentum expansion: the latter can be checked and enforced setting appropriate upper cuts on the p_T distribution. As an example, in Fig. 3, we show the prediction in the SM (left plot) and in the specific NP benchmark (right plot) of the normalized p_T-ordered double differential distribution.

6.2 Associated vector boson plus Higgs production

Higgs production in association with a W or Z boson are respectively the third and fourh Higgs production processes in the SM, by total cross section. Combined with VBF studies, they offer other important handles to disentangle the various Higgs PO. Due the lower cross section, this process is mainly studied in the highest-rate Higgs decay channels, such as $h \to b\bar{b}$ and WW^*. The drawback of these channels is the background, which is overwhelming in the $b\bar{b}$ case and of the same order as the signal in the WW^* channels. Nonetheless, kinematical cuts, such as the Higgs p_T in the $b\bar{b}$ case, and the use of multivariate analysis allow the experiments to precisely extract the the signal rates from these measurements.

An important improvement for future studies of these channels with the much higher luminosity which will be available, is to study differential distributions in some specific kinematical variables. In Section 5.1.2 we showed that the invariant mass of the Vh

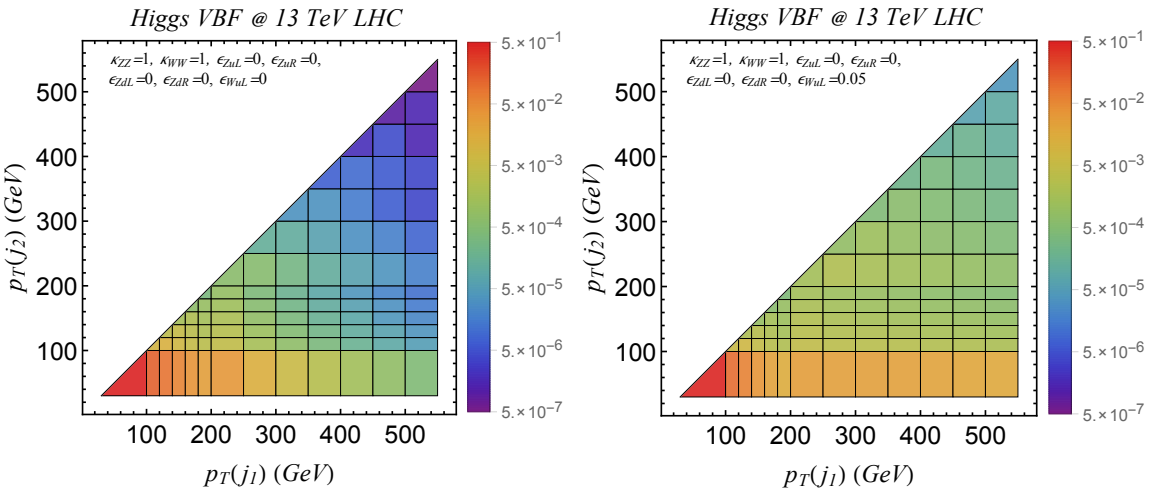

Figure 3: Double differential distribution in the two VBF-tagged jet p_T for VBF Higgs production at 13 TeV LHC. The distribution is normalized such that the total sum of events in all bins is 1. (Left) Prediction in the SM. (Right) Prediction for NP in $\epsilon_{Wu_L} = 0.05$.

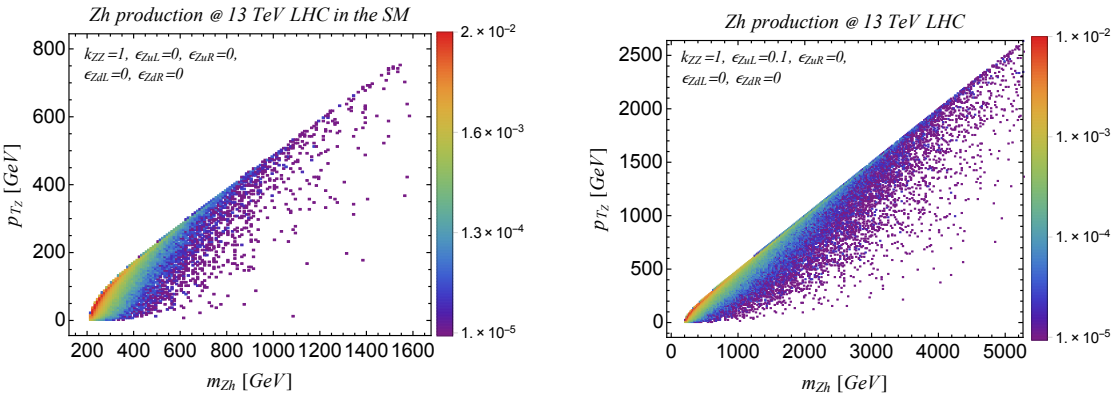

Figure 4: The correlation between the Zh invariant mass and the p_T of the Z boson in Zh associate production at the 13TeV LHC in the SM (left plot) and for a BSM point $\kappa_{ZZ} = 1$, $\epsilon_{Zu_L} = 0.1$ (right plot). A very similar correlation is present in the Wh channel.

system is the most important observable in this process, since the form factors directly depend on it. In those channels where the Vh invariant mass can not be reconstructed due to the presence of neutrinos, another observable which shows some correlation with the q^2 is the p_T of the vector boson, or equivalently of the Higgs, as can be seen in the Fig. 4. Even though this correlation is not as good as the one between the jet p_T and the momentum transfer in the VBF channel, a measurement of the vector boson (or Higgs) p_T spectrum, i.e. of some form factor $\tilde{F}^{Vh}(p_{TV})$ would still offer important information on the underlying structure of the form factors appearing in Eq. (52), $F_L^{q_i Z}(q^2)$ or $G_L^{q_{ij} W}(q^2)$. The invariant mass of the Vh system is given by $m_{Vh}^2 = q^2 = (p_V + p_h)^2 = m_V^2 + m_h^2 + 2p_V \cdot p_h$. Going in the c.m. frame, we have $p_V = (E_V, \vec{p}_T, p_z)$ and $p_h = (E_h, -\vec{p}_T, -p_z)$, where $E_i = \sqrt{m_i^2 + p_T^2 + p_z^2}$ $(i = V, h)$. Computing m_{Vh}^2 explicitly:

$$m_{Vh}^2 = m_V^2 + m_h^2 + 2p_T^2 + 2p_z^2 + 2\sqrt{m_V^2 + p_T^2 + p_z^2}\sqrt{m_h^2 + p_T^2 + p_z^2} \overset{|p_T|\to\infty}{\longrightarrow} 4p_T^2 \ . \tag{56}$$

For $p_z = 0$ this equation gives the minimum q^2 for a given p_T, which can be seen as the left edge of the distributions in the Fig. 4. This is already a valuable information, for example the boosted Higgs regime used in some $b\bar{b}$ analysis implies a lower cut on the q^2: a bin with $p_T > 300$ GeV implies $\sqrt{q^2} \gtrsim 630$ GeV, which could be a problem for the validity of the momentum expansion.

In the Wh process, if the W decays leptonically its p_T can not be reconstructed independently of the Higgs decay channel. One could think that the p_T of the charged lepton from the W decay would be correlated with the Wh invariant mass, but we checked that there is no significant correlation between the two observables.

6.3 Validity of the momentum expansion

In VBF, in order to control the momentum expansion at the basis of the PO composition, it is necessary to set an upper cut on the leading VBF-tagged jet p_T. The momentum expansion of the form factors in Eq. (49) makes sense only if the higher order terms in $q_{1,2}^2$ are suppressed. This leads to a consistency condition,

$$\epsilon_{X_f} \ q_{\max}^2 \lesssim m_Z^2 \ g_X^f \ , \tag{57}$$

where $q_{\max}^2$ is the largest momentum transfer in the process. A priori we don't know which is the size of the ϵ_{X_f} or, equivalently, the effective scale of new physics. However, a posteriori we can verify by means of Eq. (57) if we are allowed to truncate the momentum expansion to the first non-trivial terms. In practice, setting a cut-off on p_T we implicitly define a value of $q_{\max}$. Extracting the ϵ_{X_f} for $p_T^j < (p_T^j)^{\max} \approx q_{\max}$ we can check if Eq. (57) is satisfied. Ideally, the experimental collaborations should perform the extraction of the ϵ_{X_f} for different values of $(p_T^j)^{\max}$ optimizing the range according to the results obtained.

A further simple check to assess the validity of the momentum expansion is obtained comparing the fit performed including the full quadratic dependence of the distributions,

as function on the PO, with the fit in which such distributions are linearized in $\delta\kappa_X \equiv \kappa_X - \kappa_X^{\rm SM}$ and ϵ_X. The idea behind this procedure is that the quadratic corrections to physical observable in $\delta\kappa_X$ and ϵ_X are formally of the same order as the interference of the first neglected term in Eq. (49) with the leading SM contribution. If the two fits provide similar results, one can conclude that the terms neglected in PO decomposition are indeed subleasing. If the the fits yields significantly different results, the difference can be used as an estimate of the uncertainty due to the neglected higher-order terms in the momentum expansion.

- To be continued....

7 Parameter counting and symmetry limits

We are now ready to identify the number of independent pseudo-observables necessary to describe various sets of Higgs decay amplitudes and productions cross sections [this section is still to be checked/completed]

7.1 Yukawa modes

Regarding $h \to f\bar{f}$ decay modes, as discussed in Sec. 2.1 the amplitude is fully characterised by two independent PO; κ_f and $\lambda_f^{\rm CP}$. Considering only the decay channels relevant for LHC, the full set of 8 parameters is:

$$\kappa_b, \kappa_c, \kappa_\tau, \kappa_\mu, \lambda_b^{\rm CP}, \lambda_c^{\rm CP}, \lambda_\tau^{\rm CP}, \lambda_\mu^{\rm CP} \ . \tag{58}$$

Assuming in addition CP conservation, $\lambda_f^{\rm CP} = 0$ for each f, the number of PO is reduced to 4.

7.2 Higgs EW decays

As far as EW decays are concerned, we focus our attention only on leptonic channels. The neutral current processes $h \to e^+e^-\mu^+\mu^-$, $h \to e^+e^-e^+e^-$ and $h \to \mu^+\mu^-\mu^+\mu^-$, together with the photon channels $h \to \gamma\gamma$ and $h \to \ell^+\ell^-\gamma$, can be described in terms of 11 real parameters:

$$\kappa_{ZZ}, \kappa_{Z\gamma}, \kappa_{\gamma\gamma}, \epsilon_{ZZ}, \epsilon_{ZZ}^{CP}, \epsilon_{Z\gamma}^{CP}, \epsilon_{\gamma\gamma}^{CP}, \epsilon_{Ze_L}, \epsilon_{Ze_R}, \epsilon_{Z\mu_L}, \epsilon_{Z\mu_R} \tag{59}$$

(of which only the subset $\{\kappa_{\gamma\gamma}, \kappa_{Z\gamma}, \epsilon_{\gamma\gamma}^{CP}, \epsilon_{Z\gamma}^{CP}, \}$ is necessary to describe $h \to \gamma\gamma$ and $h \to \ell^+\ell^-\gamma$). The charged-current process $h \to \bar{\nu}_e e \bar{\mu} \nu_\mu$ needs 7 further independent real parameters to be completely specified:

$$\kappa_{WW}, \epsilon_{WW}, \epsilon_{WW}^{CP} \text{ (real)} \quad + \quad \epsilon_{We_L}, \epsilon_{W\mu_L} \text{ (complex)} \ . \tag{60}$$

Finally, the mixed processes $h \to e^+e^-\nu\bar{\nu}$ and $h \to \mu^+\mu^-\nu\bar{\nu}$ can be described by a subset of the coefficients already introduced plus 2 further real contact interactions coefficients:

$$\epsilon_{Z\nu_e}, \epsilon_{Z\nu_\mu} \ . \tag{61}$$

This brings the total number of (real) parameters to 20.

A first simple restriction in the number of parameters is obtained by assuming flavor universality (i.e. enlarging the flavor symmetry to the full $U(3)^5$ flavor group). In our setup this simply means assuming that the contact interactions coefficients are independent of the generations:

$$\epsilon_{Ze_L} = \epsilon_{Z\mu_L} \ , \qquad \epsilon_{Ze_R} = \epsilon_{Z\mu_R} \ , \qquad \epsilon_{Z\nu_e} = \epsilon_{Z\nu_\mu} \ , \qquad \epsilon_{We_L} = \epsilon_{W\mu_L} \ . \tag{62}$$

Since the last coefficients are complex in general, these are five relations which allow to reduce the number of parameters to 15. This assumption can be tested directly from data by comparing the extraction of the contact terms from $h \to 2e2\mu$, $h \to 4e$ and $h \to 4\mu$ modes.

The assumption that CP is a good approximate symmetry of the BSM sector and that the Higgs is a CP-even state, allows us to set to zero six independent (real) coefficients:

$$\epsilon_{ZZ}^{CP} = \epsilon_{Z\gamma}^{CP} = \epsilon_{\gamma\gamma}^{CP} = \epsilon_{WW}^{CP} = \mathrm{Im}\epsilon_{We_L} = \mathrm{Im}\epsilon_{W\mu_L} = 0 \ . \tag{63}$$

Assuming, at the same time, flavor universality, the number of free real parameters reduces to 10.

7.3 EW production processes

The additional set of PO appearing in EW production process, compared to $h \to 4\ell$ decays, is represented by the contact terms for the light quarks. In a four-flavor scheme, in absence of any symmetry assumption, the number of independent parameters for the neutral currents contact terms is 16 ($\epsilon_{Zq^{ij}}$, where $q = u_L, u_R, d_L, d_R$, and $i, j = 1, 2$): 8 real parameters for flavor diagonal terms and 4 complex flavour-violating parameters. Similarly, there are 16 independent parameters in charged currents, namely the 8 complex terms $\epsilon_{Wu_L^i d_L^j}$ and $\epsilon_{Wu_R^i d_R^j}$. However, we can strongly reduce the number of independent PO under neglecting the terms that violates the $U(1)_f$ flavour symmetry acting on each of the light fermion species, u_R, d_R, s_R, c_R, $q_L^{(d)}$, and $q_L^{(s)}$, where $q_L^{(d,s)}$ denotes the two quark doublets in the basis where down quarks are diagonal. This symmetry is an exact symmetry of the SM in the limit where we neglect light quark masses. Enforcing it at the PO level is equivalent to neglecting terms that do not interfere with SM amplitudes in the limit of vanishing light quark masses. Under this (rather conservative) assumption, the number of independent neutral currents contact terms reduces to 8 real parameters,

$$\epsilon_{Zu_R}, \ \epsilon_{Zc_R}, \ \epsilon_{Zd_R}, \ \epsilon_{Zs_R}, \ \epsilon_{Zd_L}, \ \epsilon_{Zs_L}, \ \ \epsilon_{Zu_L}, \ \epsilon_{Zc_L}, \tag{64}$$

and only 2 complex parameters are in the charged-current case:

$$\epsilon_{Wu_L^i d_L^j} \equiv V_{ij}\epsilon_{Wu_L^j}\,, \qquad \epsilon_{Wu_R^i d_R^j} = 0\ . \tag{65}$$

A further interesting reduction of the number of parameters occurs under the assumption of an $U(2)^3$ symmetry acting on the first two generations, namely the maximal flavor symmetry compatible with the SM gauge group. The independent parameters in this case reduces to six:

$$\epsilon_{Zu_L},\ \epsilon_{Zu_R},\ \epsilon_{Zd_L},\ \epsilon_{Zd_R},\ \epsilon_{Wu_L}\ , \tag{66}$$

where ϵ_{Wu_L} is complex, or five if we further neglect CP-violating contributions (in such case ϵ_{Wu_L} is real). We employ this set of assumptions ($U(2)^3$ flavor symmetry and CP conservation) in the phenomenological analysis of VBF and VH processes discussed in the rest of the paper. The last symmetry hypothesis that can be enforced is custodial symmetry, that implies the relation

$$\epsilon_{Wu_L} = \frac{c_W}{\sqrt{2}}(\epsilon_{Zu_L} - \epsilon_{Zd_L})\ , \tag{67}$$

reducing the number of independent PO to four in the $U(2)^3$ case (independently of any assumption about CP).

8 Conclusion

Higgs (EW) decay amplitudes

Amplitudes	Flavor + CP	Flavor Non Univ.	CPV
$h \to \gamma\gamma, 2e\gamma, 2\mu\gamma$ $4e, 4\mu, 2e2\mu$	$\kappa_{ZZ}, \kappa_{Z\gamma}, \kappa_{\gamma\gamma}, \epsilon_{ZZ}$ $\epsilon_{Ze_L}, \epsilon_{Ze_R}$	$\epsilon_{Z\mu_L}, \epsilon_{Z\mu_R}$	$\epsilon^{CP}_{ZZ}, \epsilon^{CP}_{Z\gamma}, \epsilon^{CP}_{\gamma\gamma}$
$h \to 2e2\nu, 2\mu2\nu, e\nu\mu\nu$	$\kappa_{WW}, \epsilon_{WW}$ $\epsilon_{Z\nu_e}$, $\mathrm{Re}(\epsilon_{We_L})$	$\epsilon_{Z\nu_\mu}$, $\mathrm{Re}(\epsilon_{W\mu_L})$ $\mathrm{Im}(\epsilon_{W\mu_L})$	ϵ^{CP}_{WW}, $\mathrm{Im}(\epsilon_{We_L})$

Higgs (EW) production amplitudes

Amplitudes	Flavor + CP	Flavor Non Univ.	CPV
VBF neutral curr. and Zh	$[\ \kappa_{ZZ}, \kappa_{Z\gamma}, \epsilon_{ZZ}\ ]$ $\epsilon_{Zu_L}, \epsilon_{Zu_R}, \epsilon_{Zd_L}, \epsilon_{Zd_R}$	$\epsilon_{Zc_L}, \epsilon_{Zc_R}$ $\epsilon_{Zs_L}, \epsilon_{Zs_R}$	$[\ \epsilon^{CP}_{ZZ}, \epsilon^{CP}_{Z\gamma}\ ]$
VBF charged curr. and Wh	$[\ \kappa_{WW}, \epsilon_{WW}\ ]$ $\mathrm{Re}(\epsilon_{Wu_L})$	$\mathrm{Re}(\epsilon_{Wc_L})$ $\mathrm{Im}(\epsilon_{Wc_L})$	$\mathrm{Im}(\epsilon_{Wu_L})$

EW production and decay modes, with custodial symmetry

Amplitudes	Flavor + CP	Flavor Non Univ.	CPV
production & decays	$\kappa_{ZZ}, \kappa_{Z\gamma}, \epsilon_{ZZ}$		$\epsilon^{CP}_{ZZ}, \epsilon^{CP}_{Z\gamma}$
VBF and VH only	$\epsilon_{Zu_L}, \epsilon_{Zu_R}, \epsilon_{Zd_L}, \epsilon_{Zd_R}$	$\epsilon_{Zc_L}, \epsilon_{Zc_R}$ $\epsilon_{Zs_L}, \epsilon_{Zs_R}$	
decays only	$\kappa_{\gamma\gamma}, \epsilon_{Ze_L}, \epsilon_{Ze_R}$, $\mathrm{Re}(\epsilon_{We_L})$	$\epsilon_{Z\mu_L}, \epsilon_{Z\mu_R}$	$\epsilon^{CP}_{\gamma\gamma}$

References

[1] D. Y. Bardin, M. Grunewald and G. Passarino, hep-ph/9902452.

[2] G. Passarino, C. Sturm and S. Uccirati, Nucl. Phys. B **834** (2010) 77 arXiv:1001.3360 [hep-ph].

[3] M. Gonzalez-Alonso, A. Greljo, G. Isidori and D. Marzocca, Eur. Phys. J. C **75** (2015) 128 arXiv:1412.6038 [hep-ph].

[4] M. Gonzalez-Alonso, A. Greljo, G. Isidori and D. Marzocca, Eur. Phys. J. C **75** (2015) 341 arXiv:1504.04018 [hep-ph].

[5] M. Ghezzi, R. Gomez-Ambrosio, G. Passarino and S. Uccirati, JHEP **1507** (2015) 175 arXiv:1505.03706 [hep-ph].

[6] A. David and G. Passarino, arXiv:1510.00414 [hep-ph].

[7] A. Greljo, G. Isidori, J. M. Lindert and D. Marzocca, arXiv:1512.06135 [hep-ph].

[8] S. Heinemeyer *et al.* [LHC Higgs Cross Section Working Group Collaboration], arXiv:1307.1347 [hep-ph].

[9] W. Bernreuther and A. Brandenburg, Phys. Lett. B **314** (1993) 104; Phys. Rev. D **49** (1994) 4481.

[10] S. Berge, W. Bernreuther and J. Ziethe, Phys. Rev. Lett. **100** (2008) 171605 [arXiv:0801.2297]. S. Berge, W. Bernreuther and S. Kirchner, arXiv:1410.6362 [hep-ph].

[11] N. Davidson, T. Przedzinski and Z. Was, arXiv:1011.0937 [hep-ph].

[12] M. Bordone, A. Greljo, G. Isidori, D. Marzocca and A. Pattori, Eur. Phys. J. C **75** (2015) 8, 385 arXiv:1507.02555 [hep-ph].

[13] J. Alwall *et al.*, JHEP **1407** (2014) 079 arXiv:1405.0301 [hep-ph].